Supplementary material

Hyporheic exchange in recirculating flumes under heterogeneous bacterial and morphological conditions

Andrea Betterle[1,2,3]*, Anna Jaeger[4,5], Malte Posselt[6], Claudia Coll[1,6], Jonathan P. Benskin[6] and Mario Schirmer[1,2]

1 Eawag – Swiss Federal Institute of Aquatic Science and Technology, Department of Water Resources and Drinking Water, Duebendorf, Switzerland
2 University of Neuchâtel, Centre of Hydrogeology and Geothermics (CHYN), Neuchâtel, Switzerland
3 University of Trento, Department of Civil, Environmental and Mechanical Engineering, Trento, Italy
4 Leibniz-Institute for Freshwater Ecology and Inland Fisheries, Department of Ecohydrology, Berlin,Germany
5 Humboldt University Berlin, Geography Department, Berlin, Germany
6 Department of Environmental Science, Stockholm University, Stockholm, Sweden

* Correspondence: andrea.betterle@unitn.it

Contents

S1.1 Pictures of the experimental setup

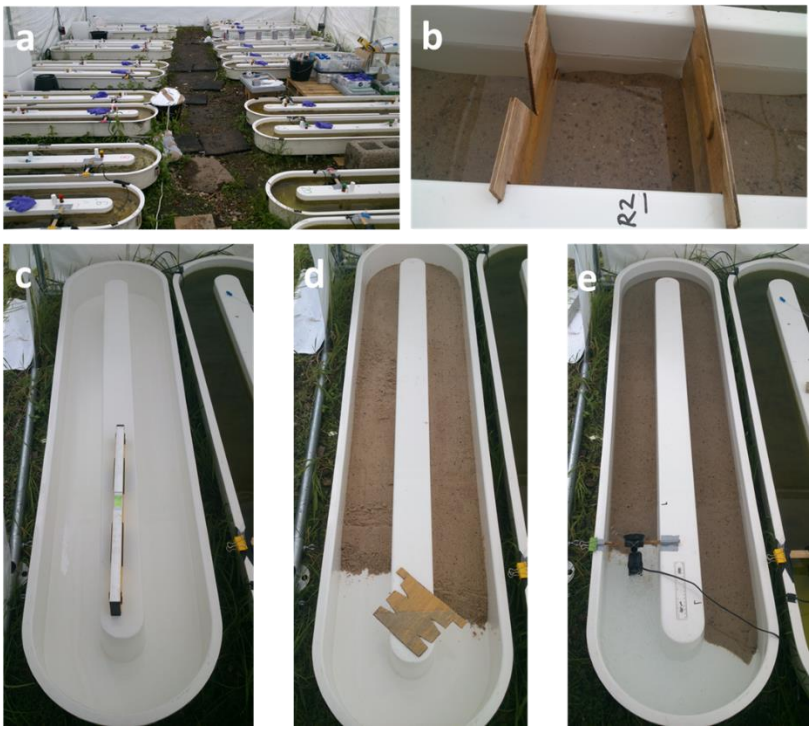

Figure SI.1: Pictures of the flume experiment. (a) overview of all flumes on day 47; (b) formation of bedforms using wooden plates; (c) leveling of an empty flume; (d) flume after filling and leveling the sediment; e) flume after filling the water and installing the pump.

SI.2 Estimate of sediment hydraulic conductivity

Figure SI.2 shows the decrease of the water level observed in the seepage device used to estimate the hydraulic conductivity of the sediments as described in Section 2.2. The falling head test was repeated four times. The four estimates of the hydraulic conductivity obtained by fitting Equation 1 to the observations resulted in an average value of $K_s=2.35\cdot10^{-4}$ m/s. The permeability k of the sediments accounting for the viscosity and the density of water at 17°C is $k=2.40\cdot10^{-11}$ m^2. As 17°C was representative of the average temperature in the flumes throughout the experiment (as well as during the falling head tests), no relevant deviations are expected in the hydraulic conductivity of the sediments due to temperature-induced variation in the density and viscosity of the water.

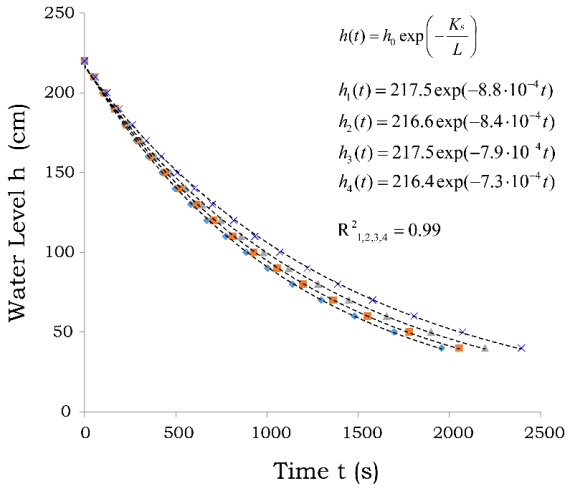

Figure SI.2: Decays of water level observed in the seepage meter used to estimate the hydraulic conductivity of the sediments during four falling head tests. The equations for the best exponential fits (dashed curves) are reported together with their general analytical expression.

SI.3 Estimate of the average surface flow velocity

Direct estimates of flow velocity can be based on the time interval required by a floating object to cover a specific distance along a flume. Although these measures can provide rough estimates of flow velocity, they are affected by two major biases. First, the presence of the dunes in the setups with 3 and 6 bedforms considerably altered the flow conditions (i.e. the flow field is disturbed and concentrated towards the surface due to the presence of the dunes). Consequently, flowrate estimates based on surface water velocity will likely be biased towards larger flowrates. Second, even in case of steady flow in a uniform channel section (i.e. absence of bedforms), flow velocity tends to be larger at the surface. This is a consequence of the shear forces acting between the flowing water and the sediments that, in turn, causes a vertical flow velocity gradient. The procedure presented in this section was developed to obtain a representative values of the average surface flowrates explicitly accounting for the aforementioned processes.

For each B0 and B3 flume, seven estimates of surface flow velocity were obtained by measuring the time interval required by a floater to cover a single side of the recirculating flume (flow measurements were performed on the 27th experimental day). For the B3 setting, the measurements were conducted on the side of the flume where no bedforms were present, whereas in case of the B0 setting the measurements were conducted on the side opposite to the pump. Overall a total of 42 flow measurements were performed for the B0 experiments and 56 for the B3 experiments. The average (± standard

deviation) surface flow velocity measures were respectively: $\overline{u}_{B0}$ = 10.0 ± 1.0 cm/s , $\overline{u}_{B3}$ = 7.5 ± 0.8 cm/s. The logarithmic vertical velocity profile in the B0 and B3 settings obtained as described in Section 2.3 is shown in Figure SI.3. Integrating the flow profile along the vertical direction, the average flow velocities are respectively: $U_{B0} = 8.7\ cm/s$ and $U_{B3} = 6.6\ cm/s$. Furthermore, by combining U_{B0} and U_{B3} as described in Section 2.3 (Equation 6), the average flow velocity in the B6 setting is $U_{B6} = 5.5\ cm/s$. In fact, due to experimental constraints, direct flow measurements were not possible in B6 settings and flow velocity had to be estimated indirectly. Note that, using Equation 2 to describe the vertical variation of the flow velocity, it is assumed that the friction between the water and the vertical walls of the flumes is negligible compared to the friction with the sediments. Although it is reasonable to assume that the vertical walls are smoother than the sandy bottom, the hypothesis might lead to slight overestimates of flow velocities.

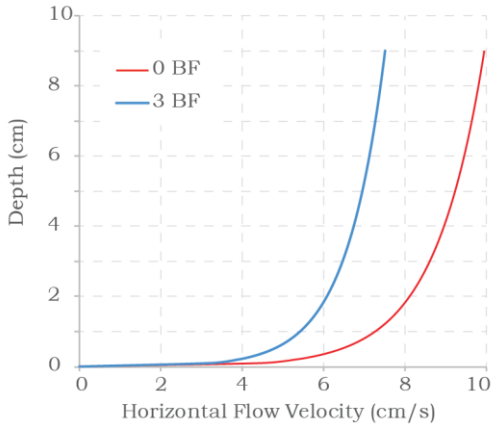

Figure SI.3: Modelled logarithmic vertical profile of flow velocity (0 and 3 bedform cases). The flow velocity profiles are obtained as described in Section 2.3.

SI.4 Breakthrough of acesulfame

Figure SI.4 shows the breakthrough curve of acesulfame at the three sampling locations A, B and C located in the first bedform of flume 18 (see Section 2.1 and 2.4). Given the negligible sorption/adsorption of acesulfame in the porous matrix, the time-to-peak of its concentration is representative for the advective travel times of water to the different sampling locations.

Because of the temporal resolution of sampling (porewater samples were taken after 0, 24, 48, 72 and 168 hours), and because of the relative fast initial breakthrough of acesulfame, it was not possible to clearly

differentiate between the times-to-peaks at the first two sampling points.

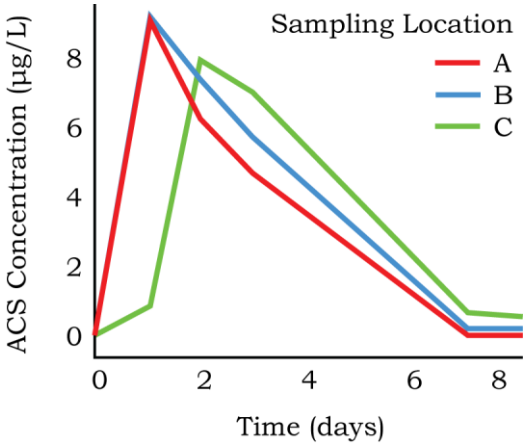

Figure SI.4: Concentration of acesulfame versus time at the three sampling points located in the first bedform of flume 18 (see Figure 2). From the time-to-peak of the break through it is possible to infer the travel time of water parcels through the sediments.

SI.5 Summary of the salt dilution tests

Figure SI.5 summarizes the results obtained from the salt dilution tests specifically for each experimental flume (Section 3.1 and Figure 3). The figure shows the hyporheic exchange fluxes, the exchange volume and the mean residence time in the sediments as described in Section 2.5. Figure SI.5 highlights a clear inter-flume variability between the experimental replicates.

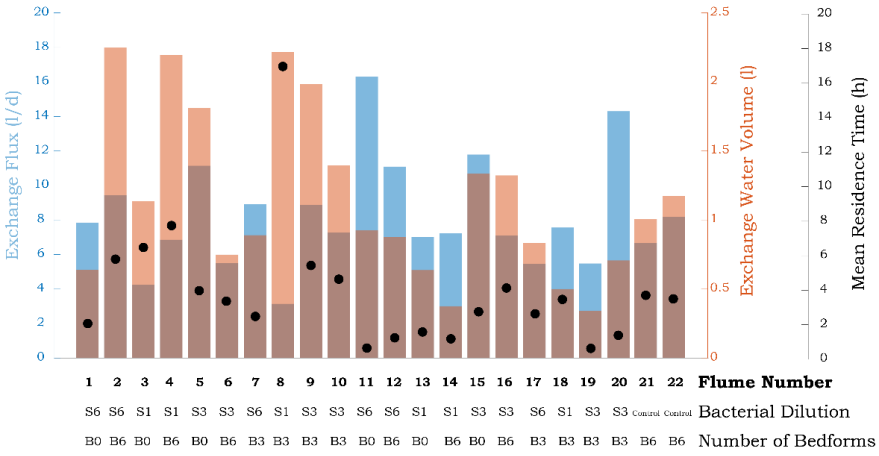

Figure SI.5: Exchange fluxes (blue bars), exchange water volumes (orange bars), and mean residence times (black dots) in the sediments estimated by means of the salt dilution tests for each experimental flume.

SI.6 Distribution of the flow path lengths

The histograms in Figure SI.6 show the modeled distribution of the lengths of the flow paths reaching the three sampling locations in the B3 and B6 case. Results are additionally modulated based on the bedform order (i.e. first or second bedform). The sampling locations (A, B and C) and the bedforms (1st and 2nd) are progressively coded starting from upstream. Figure SI.6 shows that – for a given bedform – the average flow path length is similar in the B3 and in the B6 settings (i.e. it does not depend on the average surface flowrate). Moreover, flow path lengths display little variability in the B3 versus the B6 settings as well as for the 1st versus the 2nd bedform.

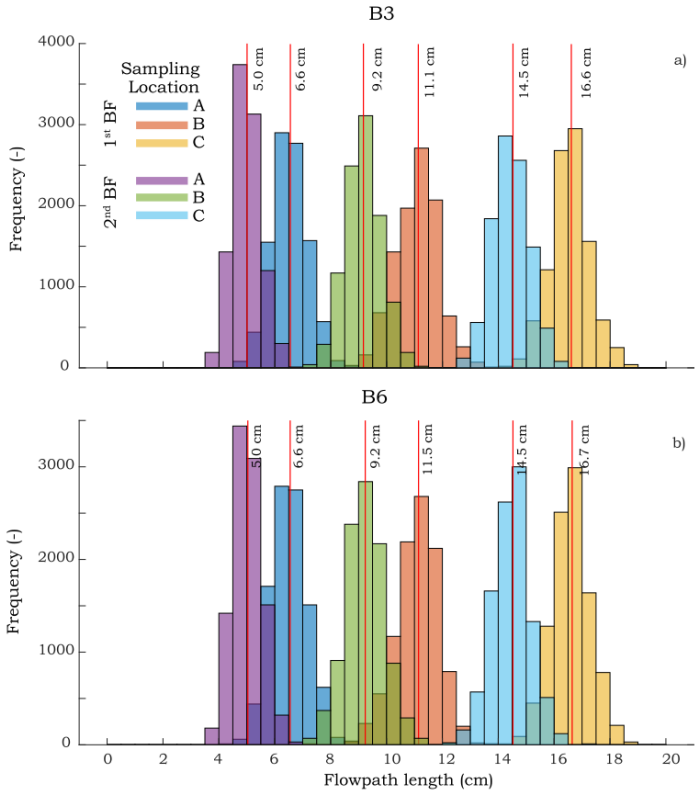

Figure SI.6: Frequency distribution of the flow path length calculated by backtracking the water parcels starting from the three sampling locations in the first and in the second bedforms for settings B3 (a) and B6 (b). The mean values of the distributions are reported in correspondence with the (thin) red lines.

SI.7 Modelling the coupled surface–subsurface hyporheic exchange during the final experimental phase

Throughout the experiment, the initial morphology of the streambed described in Section 2.1 has been progressively smoothed by the persistent surface flow. During the final phase of the experiment

(when salt dilution tests were performed, see Section 2.5 and 3.1) the amplitude of the bedforms in the B3 and B6 experimental setup reduced of about 20 % (≈1.5 cm).

Figure SI.7a) shows the couple surface-subsurface flowfield in B6 settings where the sediment interface mimics the final streambed morphology. The flowfield is modeled for the B6 scenarios because they were the only cases where surface flow velocity measurements were available at the final experimental phase. Specifically, average surface flowrate estimated as described in Section 2.3 based on surface velocity measurements taken during the final experimental period reads: $U_6^{final} \approx 4\ cm/s$. The remaining modelling parameters are set as described in Section 4.

In this case, the reduced prominence of bedforms results in lower hyporheic exchange, as well as in a less heterogeneous velocity flow filed (Figure SI.7a).

Figure SI.7b) displays the longitudinal exchange profile (i.e. the flow velocity perpendicular to the sediment-water interface). The total exchange flux computed as described in Section 5.1 reads: $Q_{B6\,final}^{model} = 8.8\ l/d$. The numerically-estimated exchange flux corresponds to the exchange obtained from the salt dilution tests in case of low bacterial diversity ($Q_{B6,S6}^{s.d.t.} = 9.0\ l/d$, see Table 2a).

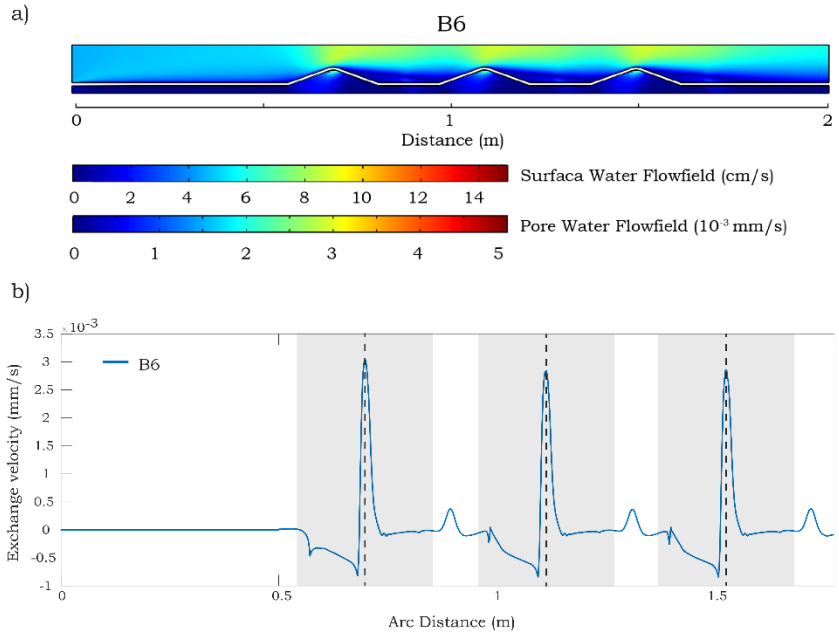

Figure SI.7: a): Coupled surface water and pore water flowfield in B6 settings. Model domain reproduces the sediment morphology observed during the final phase of the experiment (bedform amplitude reduced of about 20%). b): hyporheic pattern (normal flow) at the sediment-water interface. Positive (negative) values correspond to upwelling (downwelling). The position of the bedforms (and bedform crests) are identified by the gray shaded areas (and dashed lines).

SI.8 Notation

Table SI.1: Table summarizing the notation employed in the study

B0, B3, B6	Labels denoting the 3 morphological configurations of the sediments in the flumes
S1, S3, S6	Labels denoting the 3 dilution ratio of the river Erpe sediments (represent different levels of bacterial diversity)
K_s	Saturated hydraulic conductivity of the sediments
k	Permeability of the sediments
n	Porosity of the sediments
ρ	Density of water
ν	Kinematic viscosity of water
μ	Dynamic viscosity of water
u(y)	Vertical profile of the horizontal flow velocity
$\bar{u}$	Maximum water flow velocity at the water-atmosphere interface
U	Average horizontal flow velocity
u_τ	Shear velocity
τ_w	Shear stress at the sediment-water interface
K, C^+	Hydrodynamic coefficients
E	Hydrodynamic energy losses
Re	Reynolds number
D	Hydraulic radius of the flumes
α, β	Scaling parameters relating the flow velocity to the hydrodynamic energy losses in the flumes
C(t), C_{eq}, C_0	Electrical conductivity at time t, at t=0 and at equilibrium (t=∞)
V_s, V_w	Volume of porewater affected by hyporheic exchange and volume of surface water
t_{ex}	Average residence time in the sediment estimated by means of the salt dilution tests
β_F	Forchheimer drag coefficient